EUROTHERM

UIT
Unione Italiana
Termofluidodinamica

# 2nd European Thermal-Sciences and 14th UIT National Heat Transfer Conference 1996

Proceedings of the 2nd European Thermal-Sciences
and
14th UIT National Heat Transfer Conference
Rome, ITALY, 29-31 May, 1996

**Editors**

**G.P. Celata**
ENEA, Energy Department
CR Casaccia, Rome, ITALY

**P. Di Marco**
Pisa University, Energy Department
Pisa, ITALY

**A. Mariani**
ENEA, Energy Department
CR Casaccia, Rome, ITALY

## Volume 1

1996
Edizioni ETS
PISA

# EVAPORATION AND CONDENSATION HEAT TRANSFER AND PRESSURE DROP OF R-22 INSIDE MICROFIN TUBES

**S. Arosio, A. Muzzio, A. Niro**

Dipartimento di Energetica, Politecnico di Milano
piazza Leonardo da Vinci, 32 - 20133 Milano, Italy

ABSTRACT

**In-tube flow boiling and condensation experiments for Refrigerant-22 have been carried out on two microfin tubes of differing internal profile, and on a smooth tube. All the tubes have an outer diameter of 9.52 mm. Data are for mass flow rates ranging from 5.5 to 25 g/s. In boiling tests, the nominal saturation temperature is 5 °C, with inlet vapor quality varying from 0.2 to 0.6 and quality change between the test section inlet and outlet from 0.1 to 0.5. In condensation, results are for a saturation temperature equal to 35 °C, with inlet and outlet qualities of 0.8 and 0.2, respectively. Both microfin tubes show a substantial increase in the heat transfer coefficient with respect to the smooth tube, penalised by a small increase of pressure drops. The enhancement factor turned out to be decreasing with increasing mass flow rates. Results for the smooth tube are compared with predictions of several existing correlations; experimental data agree very well with values predicted by some of such correlations.**

## 1. INTRODUCTION

Heat transfer coefficients for in-tube evaporation and condensation of halocarbon refrigerants are often low enough to represent a significant thermal resistance in heat exchange equipments for refrigeration and air-conditioning applications. Due to an emphasis on energy and materials saving considerations, many techniques for heat transfer enhancement, as discussed by Bergles in [1], may be used to produce more efficient evaporators and condensers. Any enhancement technique, however, is penalised by an increase in pressure drops. In recent years, microfin tubes, i.e., tubes having many fine helical fins on the inner surface, have received increasing attention because they can substantially enhance convective heat transfer with a small pressure drop increment. For instance, Schlager et al. in [2] and Thome in [3] list more than 20 papers that report on experimental results with halo-carbons refrigerants in microfin tubes.

Lately, many efforts have been spent in researching and developing fin shapes which provide high heat transfer coefficients and low pressure drop increases. Due to the larger complexity of fluid-dynamics and heat transfer processes involved in evaporation and condensation inside microfin tube, however, heat transfer predictions are much more difficult than for a smooth tube and, therefore, the development of more efficient fin shape is an empirical art yet. Although advances have been made in predictive methods as discussed by Webb in [4], there is a large demand for a deeper understanding of boiling and condensation mechanisms inside microfin tubes, as well as for correlations and models which predict the heat transfer and friction characteristics.

The aim of this study is to collect data on flow-boiling and convective condensation of halocarbon refrigerants inside horizontal microfin tubes. This paper reports on average heat transfer coefficients and pressure drops in convective boiling and condensation of Refrigerant-22 (R-22) inside two microfin tubes and a smooth tube, used as the reference case, with an outer diameter of 9.52 mm.

Experimental results are compared with the estimates obtained by several available correlations. The Pierre, the Saha, the Kandlikar, and the Gungor-Winterton correlations are considered for heat transfer coefficient data in flow-boiling conditions, whereas condensation data are correlated using the Shah and the Cavallini-Zecchin correlations, and the calculation schemes proposed by Butterworth and by Paikert. Finally, the pressure drop data are correlated using the correlations proposed by Chawla, Grønnerud, Friedel (only for boiling data) and Rohsenow (only for condensation data). A satisfactory agreement has been found with predictions of the correlations proposed by Pierre, by Kandlikar, by Cavallini-Zecchin, by Paikert, and by Chawla and by Grønnerud.

## 2. APPARATUS AND TEST PROCEDURES

The schematic diagram of the experimental apparatus is shown in Fig. 1. The apparatus consists of three circuits, namely, a sealed refrigerant (R-22) circuit, a water circuit to heat or cool refrigerant in the test sec

tion, and a chilled coolant (water-glycol solution) circuit. The refrigerant circuit mainly consists of a boiler, the test section, a condenser, a gear pump and a filter dryer. Boiler is a 58 $dm^3$ volume, stainless-steel pressure vessel of cylindrical shape with welded ellipsoidal heads; a heater, consisting of three electrical cartridges of 1, 1.5 and 2.5 kW power, respectively, fitted on one plug, is mounted on the boiler bottom.

Liquid and vapor are drawn from the boiler through two distinct lines. On each line two float-type flowmeters, whose float is magnetically coupled to the indicating scale, are installed to measure the volume flow rates of refrigerant stream. In order to provide a single phase flow through flowmeters for any operating conditions, a concentric-tube subcooler and a ribbon electrical heater are located upstream of the flowmeters on the liquid and vapor lines, respectively. The liquid and vapor flow rates are controlled by precision metering valves. Downstream of the valves, vapor is mixed with liquid; the two-phase mixture flows through a 1.5 m long calming section and then enters the test section. At the exit, refrigerant flows through a second calming section of 1.8 m length and then is discharged to the condenser, which provides to condensate vapor and to maintain the test section outlet pressure at a given value.

The condenser is a pressure vessel of the same shape and dimension as the boiler; three round coil heat exchangers, through which the chilled coolant is circulated, are located inside the upper part of condenser; an electrical cartridge of 1 kW power is mounted on a plug fitted on the condenser bottom. Finally, liquid refrigerant is drawn from the condenser by a gear pump and is conveyed through a filter dryer to the boiler. An other concentric-tube heat exchanger is mounted on the pump suction line to ensure a liquid flow through the pump. Refrigerant temperature is measured upstream of the flowmeters, downstream of the controlling valves, and at the inlet and outlet of the test section by thermocouples inserted in 60 mm long, 3 mm o.d., stainless steel wells located on the duct axis.

The test section is a straight, 2.6 m long, 9.52 mm o.d., copper tube that is divided in two equal parts, which we refer to as the subsections. They are connected to each other and to the loop, without any discontinuity in the duct internal diameter, via three 3-way 12-mm tee fittings. Two pressure-taps are cut in each junction; a gap between fitting inner surface and tube outer surface serves as a pressure annular-chamber; the branch of each fitting provides connection via a manifold to pressure transducers. Refrigerant pressure is measured at either the test section inlet or outlet by a strain gauge transducer, whereas an inductive transducer allows to measure pressure drops along the test section. For every subsection, wall temperature is measured in four points, namely, in two axial locations, both 140 mm from either end, and in two circumferential positions 180 degrees apart for each location, by means of T-type thermocouples which are cemented in longitudinal grooves cut in the outside wall of the tube.

Numerical simulation indicated that error in the inside wall temperature should be negligible. Every subsection is enclosed by 14 mm i.d. brass tube to provide an annulus through which the heating or cooling medium (water) is circulated. Such a jacket is mounted on subsection via two tee fittings which also allow the water to enter and leave the annulus. The distance between the inlet and discharge ducts of the jacket is 1.12 m and it is defined as the subsection active heat transfer length. Calming and test sections are insulated by a 10 cm thick, glass-wool annulus, whereas a 2 cm thick, foam plastic sheets or annulus are used for the other circuit components and pipes.

The water circuit consists of a tank provided with a heater, a centrifugal pump, the jackets surrounding the

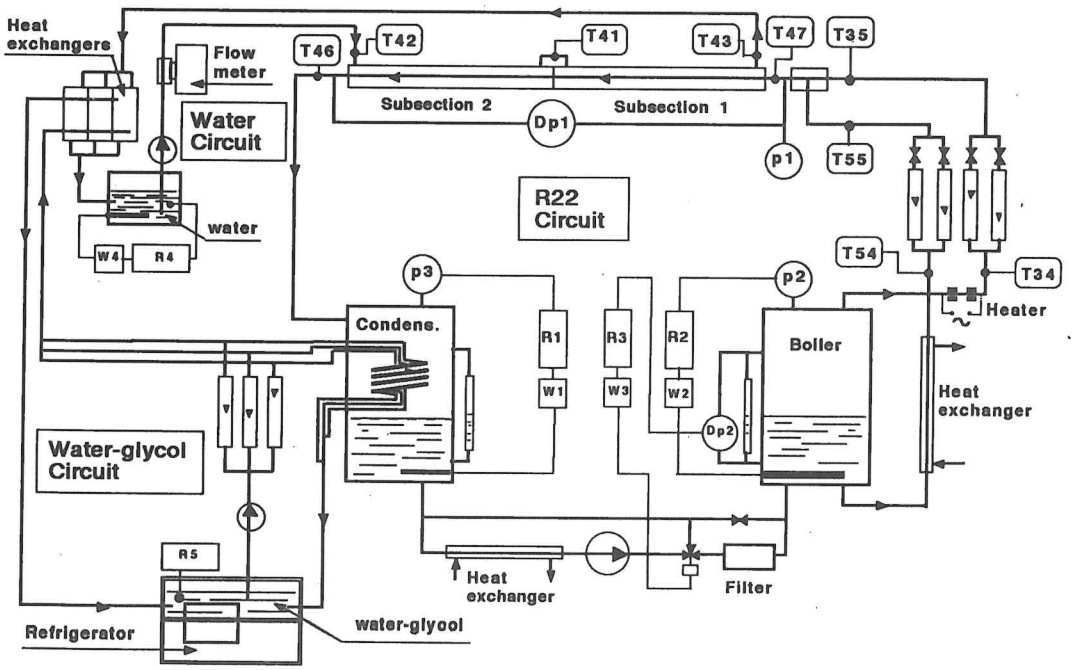


Figure 1. Schematics of the experimental apparatus.

test section, a water-to-water heat exchanger. Demineralized water is drawn from a 30 $dm^3$, stainless steel thank on which bottom a 5 kW-power heater is mounted, and it is pumped to the jackets surrounding the test section in counterflow with refrigerant. At the last jacket exit, water flows through a plate heat exchanger in countercurrent with the chilled coolant, and then it is discharged into the thank. The water volume flow rate is measured by an inductive flowmeter. At the first subsection inlet and outlet, and at the second subsection exit the bulk temperature of water stream is measured by three thermal probes. Each such a probe consists of three T-type, thermocouples which are connected in series and separately cemented in wells drilled in a 13 mm o.d., 20 mm high, copper cylinder. A 100 Ω Pt-resistor is employed to measure the water temperature in the thank. Finally, the chilled coolant circuit is filled with a water-glycol solution and consists of a commercial refrigeration unit and a centrifugal pump. Such a circuit provides the cold medium used in the refrigerant condenser and in heat exchangers mounted both on refrigerant and water circuits.

Before refrigerant was charged into the circuit, the loop was cleaned by circulating Refrigerant-11 for three hours. Subsequently, R11 was discharged and the circuit was dried through a nitrogen flow. Loop was then evacuated using a vacuum pump, in order to eliminate gases and moisture, and it was charged with R-22.

Thermocouple voltages and signals from pressure transducers and inductive flowmeter are cyclically read by a data acquisition unit HP3497, and sent to an online PC. In order to all measurements are affected by similar RMS relative errors, measurements of the refrigerant temperature and pressure at the test section inlet, as well as of the pressure drops and the water flow rate are based on 30, 50, 50 and 100 readings for cycle, respectively. Furthermore, every experimental data is obtained by averaging measurements from 10 cycles to reduce the influence of random errors and fluctuations.

Temperatures are converted from thermocouples voltages with experimental calibration curves specifically and preliminary obtained. Also, calibration curves of the water and refrigerant flowmeters were preliminary checked through mass and thermal power measurements, respectively. As a result of such checks, we estimate that volume flow rates of the refrigerant and water are measured with relative errors smaller than 2% and 1%, respectively, which agree with instrument nominal accuracy. Furthermore, agreement between the wall temperatures, the refrigerant inlet and outlet temperatures and the saturation temperature corresponding to the test section pressure, was checked upon setting a refrigerant two-phase stream flowing in thermal equilibrium with a water stream at environmental temperature. As a consequence, zero off-set of the absolute pressure transducer was lightly adjusted. Finally, thermal resistance of the test section insulation was measured finding a value of about 4 K/W.

The system start-up consists of the following main procedures. At first, refrigeration unit is started. As water-glycol solution is cooled, the condenser and boiler pressures are set to values about 0.2 MPa smaller and higher than the test nominal pressure, respectively. At the same time, water temperature is set to a value 2-4 K higher or smaller than the test nominal temperature, depending on test will performed either in evaporation or condensation. As such values are attained, the mass flow rates of liquid and vapor of R-22 through the test section, as well as of water through the jackets are imposed. For the latter mass flow rate, we choose the value allowing a water temperature drop along the test section no smaller than 2 K. Finally, through many fine adjustments the steady-state condition is achieved at fixed values of temperature, inlet quality and quality change. Because accurate and reproducible data are obtained only if steady-state conditions have been really attained, on empirical basis we assumed to operate steadily when fluctuations of heat flow rate is less than one per cent. Steady-state conditions usually requires about 2.5 hours to be established after system start-up; however, this time reduces to 1.5 hours if system is already "warm".

As system operates steadily, measurement cycles start. For every operating condition, we collect at least ten experimental data (each resulting by averaging measurements from 10 cycles) with a test run time of about 60 minutes. If during a data collection steady-state condition fails, the measurement cycle is interrupted and the results logged in that cycle are rejected. At the end of every cycle, the collected experimental data are processed and quantities as mass flow rate, inlet quality, heat flow rate and heat transfer coefficients are computed. Here, we will briefly describe how heat transfer coefficient is calculated. We assume that the refrigerant temperature varies linearly between the value $T_{in}$ measured at the test section inlet, and the exit value $T_{out}$ computed as $T_{sat}[p_{sat}(T_{in}) - \Delta p]$, where $\Delta p$ is the pressure drop measured along the test section. Then, for every subsection we compute the average refrigerant temperature $T_i$, the average wall temperature $T_{w,i}$, the temperature mean difference $\Delta T_i = (T_{w,i} - T_i)$, and the heat transfer coefficient $h_i = Q_i / (A_n \Delta T_i)$ where $Q_i$ and $A_n$ are the heat flow rate and tube surface area, based on the nominal inner diameter, respectively. Average heat transfer coefficient of the test section is eventually obtained by averaging coefficients $h_i$.

Finally, experimental uncertainties for the present investigation are summarised in what follows. Pressure drop measurements are affected by an uncertainty equal to the accuracy of the differential transducer (200 Pa). The other relevant variables, instead, are characterised by the following representative values of relative uncertainty obtained through a propagation error analysis: ±2.8% for the refrigerant mass flow rate, ±1.3% for the inlet quality, ±1.4% for the heat rate, and ±7% for the average heat transfer coefficient.

## 3. EXPERIMENTAL RESULTS

The first test run performed on the equipment was entirely in the subcooled region with the smooth tube. This provided a brief check on the experimental procedure reliability and data validity. Indeed, experimental values for the forced convection heat transfer coefficient were within 5 per cent of the values determined by Gnielinski correlation with the entrance correction factor derived by Hausen [5]. In these test runs, energy balances on the water side and on the refrigerant side agreed within 2 per cent.

In saturated flow boiling or condensation, both pressure drop and average heat transfer coefficient for a

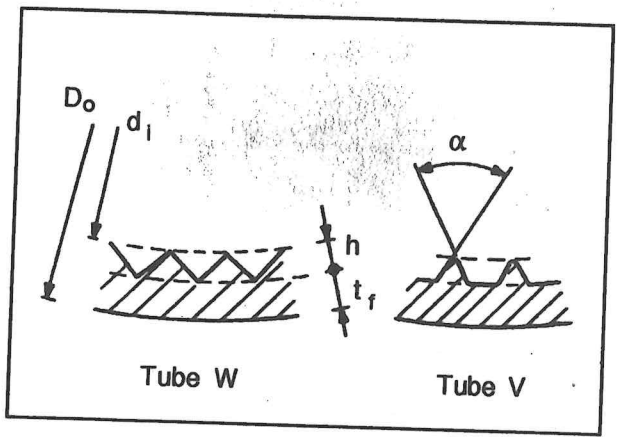


Figure 2. Drawing of the cross-sectional profile of the tested microfin tubes.

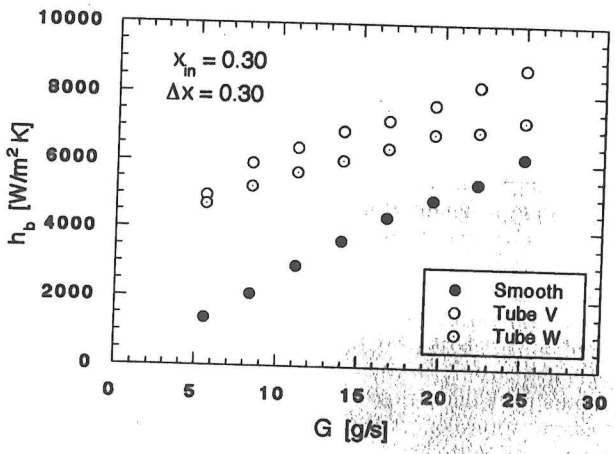


Figure 3. Evaporation heat transfer coefficient versus mass flow rate for given inlet quality and quality change.

fixed test section configuration (orientation with respect to gravity, length, dimension and shape of the cross section) depend on four independent variables, namely the total mass flow rate, the temperature or the pressure, the inlet thermodynamic quality and the heat rate. Owing to the direct proportionality between heat rate and quality change, a different but equivalent parameterization can be obtained by substituting the latter to the former in the list of independent variables.

The experimental data here reported are obtained on a smooth tube and two microfin tubes, with an outer diameter of 9.52 mm. A drawing of the microfin tubes tested is reported in figure 2 which also includes definitions of the pertinent geometric parameters. Values of these parameters, as well as smooth tube dimensions, are listed in table 1. Evaporation tests were carried out at a nominal saturation temperature of 5 °C (±0.2 K) corresponding to a pressure of 0.58 MPa, while, for condensation, the nominal temperature was 35 °C (±0.2 K) corresponding to a pressure of 1.35 MPa.

Having fixed these operating conditions, only three independent variables survive, namely, the total mass flow rate, the inlet thermodynamic quality and the quality change. In order to demonstrate clearly the effect of the variation of each variable against the others, they were varied in turn, while keeping the others constant. In evaporation tests, the total mass flow rate G ranged from 5.5 to 25 kg/s (mass flux between about 90 and 400 kg/m$^2$ s), the inlet quality $x_{in}$ was varied from 0.2 to 0.6, and the quality change $\Delta x$ from 0.1 to 0.5. In condensation only the mass flux effect was investigated in the same range as in evaporation tests, with inlet and outlet nominal qualities of 0.8 and 0.2, respectively.

Figure 3 shows evaporation heat transfer $h_b$ results plotted versus total mass flow rate G for the two microfin tubes; data obtained on the smooth tube are also included for comparison. For such tests, nominal inlet quality and quality change are $x_{in}$=0.3 and $\Delta x$=0.3. Heat transfer coefficients for microfin tubes were computed based on nominal surface area of the smooth tube. As expected, heat transfer coefficients increase with increasing mass flow rate for all the tubes, and values for microfin tubes result much higher than those for the smooth tube. Tube V appears to have the best performance but the deviation with respect to tube W is slight, being only 10 to 20 per cent. The ratio of the heat transfer coefficient of a microfin tube to that of the smooth tube, usually called [1,2] heat transfer enhancement factor, is shown in figure 4. It is apparent that the enhancement factor is decreasing with increasing mass flow rate, in agreement with the expectation that it should approach unity at very high mass flux.

For fixed mass flow rate and quality change (G=13.9 kg/s, $\Delta x$=0.3), the effect of average vapor quality $x_m$ on evaporation heat transfer coefficient can be seen on the

| Parameter \ Tube | Smooth | W | V |
|---|---|---|---|
| $D_o$ [mm] | 9.52 | 9.52 | 9.52 |
| $d_i$ [mm] | 8.92 | 8.54 | 8.52 |
| $t_f$ [mm] | 0.30 | 0.34 | 0.30 |
| h [mm] | | 0.15 | 0.20 |
| α | | 90° | 53° |
| Number of grooves | | 65 | 60 |
| Helix angle | | 25° | 18° |

Table 1: Geometric parameters of the tested tubes.

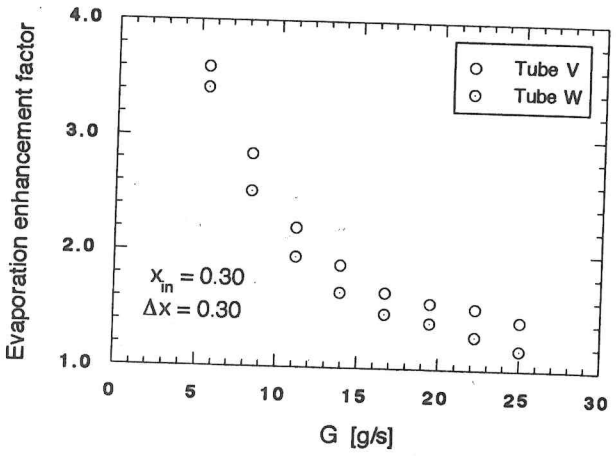


Figure 4. Evaporation enhancement factor versus mass flow rate for given inlet quality and quality change.

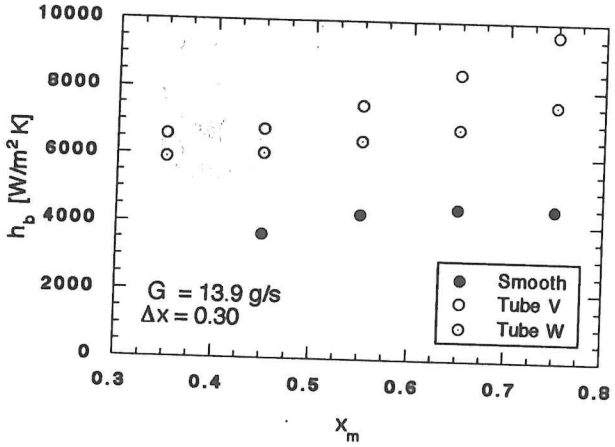


Figure 5. Evaporation heat transfer coefficient versus average vapor quality for given mass flow rate and quality change.

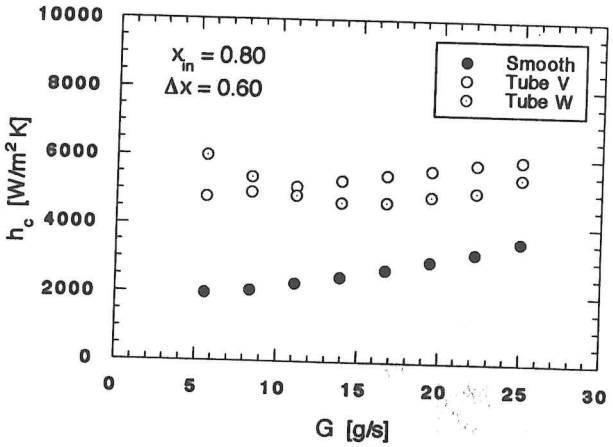


Figure 7. Condensation heat transfer coefficient versus mass flow rate for given inlet quality and quality change.

plot of figure 5. For the smooth tube, a slightly marked maximum is observed, approximately located at $x_m$=0.7. With local heat transfer coefficients, the occurrence of a maximum, more or less pronounced depending on mass flux, is well established in the relevant literature at vapor quality between 0.8 and 0.9. The sharp decrease of heat transfer coefficient after the maximum is attributable to the dryout. In the case of average heat transfer coefficients, the averaging process over a quality interval causes a curve flattening and a displacement of the maximum toward lower quality values. For the microfin tubes, a continuously increasing trend can be noticed; hence, it can be inferred that micro finning provides a shift of dryout in the region of higher quality in addition to a substantial heat transfer enhancement. Figure 6 shows the influence of quality change on heat transfer coefficients, having fixed mass flow rate and average quality (G=13.9 g/s and $x_m$=0.45). For all the tubes, heat transfer coefficients increase with increasing Δx.

Condensation results for inlet and outlet vapor qualities of 0.8 and 0.2, respectively, are shown in figure 7. As in evaporation, a substantial heat transfer improvement is achieved by the microfin tubes with respect to the smooth tube, and the corresponding heat transfer enhancement factor, shown in figure 8, is less than in evaporation at very low G, more at higher, and the same at intermediate G values. For both the smooth tube and the tube V, heat transfer coefficient increases with increasing mass flow rate, whereas tube W exhibit a peculiar trend with a marked minimum for a mass flow rate of about 15 g/s. A possible explanation can be probably found in terms of surface-tension forces that, in conjunction with the fin profile which is characterised by a sharp tip, could promote an effect like to the Gregorig's [6]. Thus, only for sufficiently large values of mass flux, shear stress forces become predominant and heat transfer coefficient starts to increase with increasing mass flow rate.

Figures 9-11 present evaporation pressure drop results obtained in the same conditions reported in figures 3, 5 and 6. As expected for all the tubes, pressure drop increases with increasing mass flow rate, or vapor quality, or quality change. However, the influence of the latter parameter is weak. The microfin tubes display an increase of pressure drops compared to the smooth tube. The increase is larger with tube V than with tube W; for the latter tube it is of the order of 10 per cent whilst, for the former, it ranges between 40 per cent and 10 per cent growing weakly as mass flow rate is increased. In

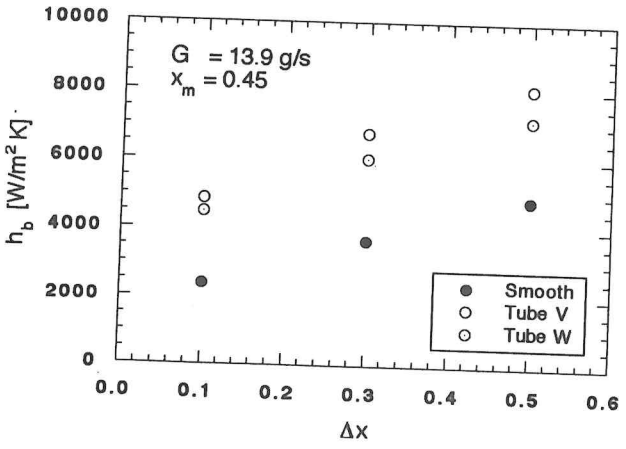


Figure 6. Evaporation heat transfer coefficient versus quality change for given mass flow rate and average vapor quality.

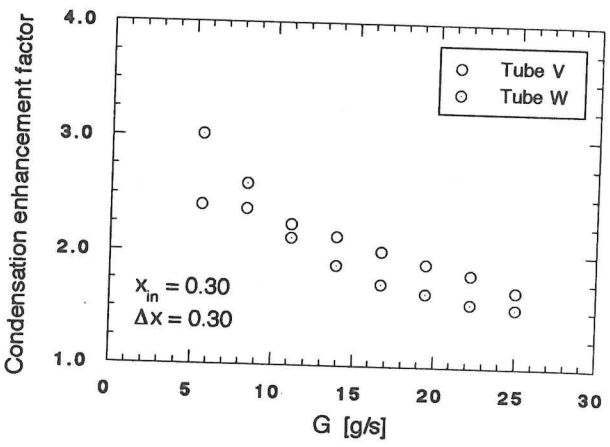


Figure 8. Condensation enhancement factor versus mass flow rate for given inlet quality and quality change.

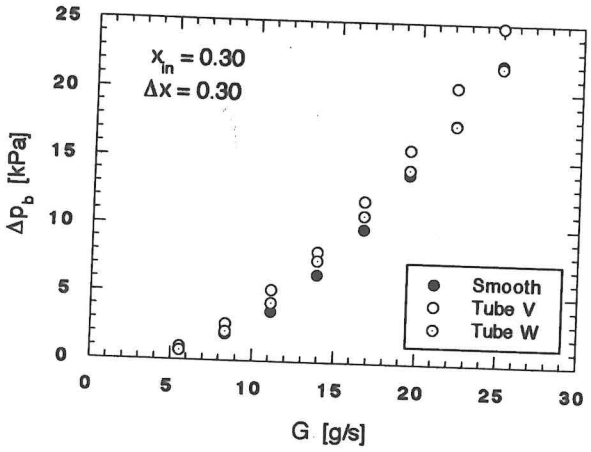


Figure 9. Evaporation pressure drop versus mass flow rate for given inlet quality and quality change.

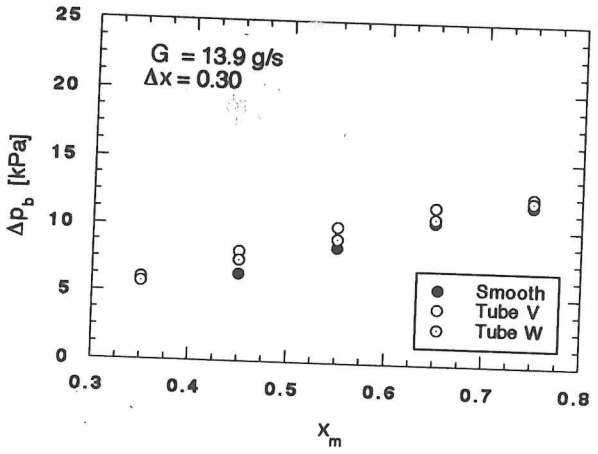


Figure 10. Evaporation pressure drop versus average vapor quality for given mass flow rate and quality change.

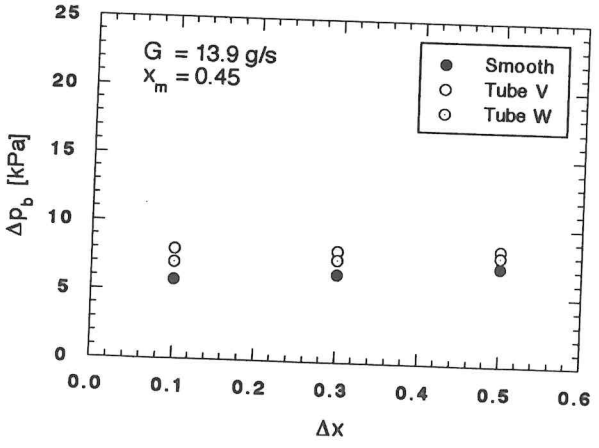


Figure 11. Evaporation pressure drop versus quality change for given mass flow rate and average vapor quality.

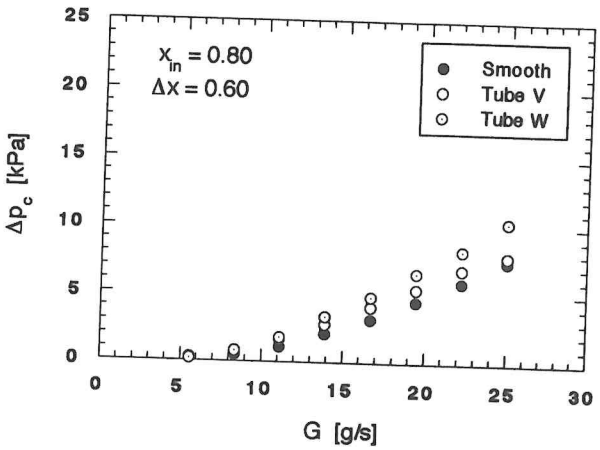


Figure 12. Condensation pressure drop versus mass flow rate for given inlet quality and quality change.

figure 12, pressure drops measured in condensation are plotted versus mass flow rate. As in evaporation, pressure drops in microfin tubes are larger than those in the smooth tube; however, the increase of pressure drops with mass flow rate varies from 60 to 30 per cent in tube W, and from 50 to 10 per cent in tube V.

Furthermore, experimental results on the smooth tube were compared with the predictions of several correlations from the literature. When using local correlations, both the average heat transfer coefficient and the pressure drop were computed by numerical integration. Computation is based on the experimental values of heat rate with the assumption of uniform heat flux in each subsection, which is tantamount to assume linear variation of the vapor quality along the subsection. The wall temperature data were not taken into account. In evaluating the total pressure drop, the accelerational term was computed on the basis of the homogeneous model, if not otherwise stated by the particular correlation.

Figure 13 shows the comparison of experimental and predicted heat transfer coefficients plotted versus mass flow rate for evaporation tests. Predictions were made through the correlations of Pierre [7], that provides average heat transfer coefficients, Chawla [8], Liu and

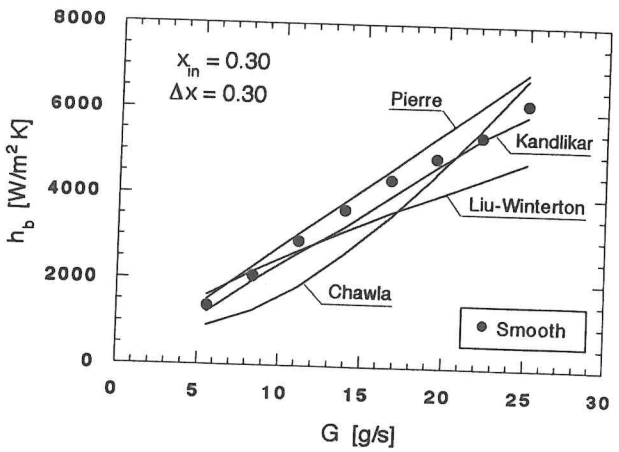


Figure 13. Comparison of experimental and predicted heat transfer coefficients for flow-boiling in the smooth tube.

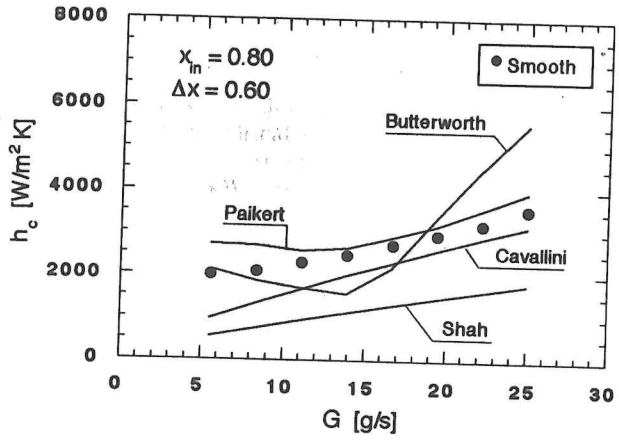


Figure 14. Comparison of experimental and predicted heat transfer coefficients for convective-condensation in the smooth tube.

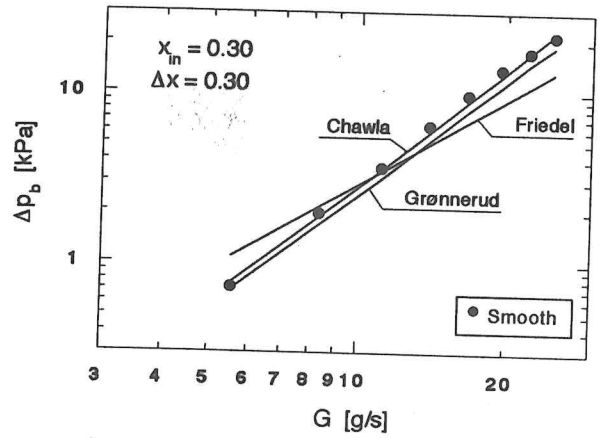


Figure 15. Comparison of experimental and predicted pressure drops for flow-boiling in the smooth tube.

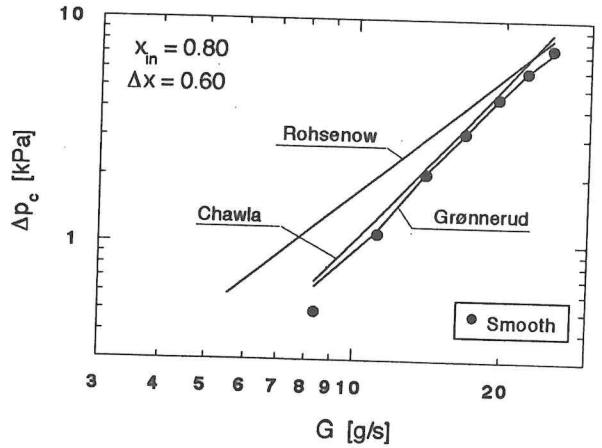


Figure 16. Comparison of experimental and predicted pressure drops for convective-condensation in the smooth tube.

Winterton [9], and Kandlikar [10] in the form recommended for refrigerants. As can be noticed, the agreement with predictions of the Pierre and the Kandlikar correlations is particularly satisfying. The condensation heat transfer results were compared with the correlations of Shah [11], Cavallini and Zecchin [12], Butterworth [13] and Paikert [14]. As shown in figure 14, the Shah correlation consistently underestimates experimental values of the heat transfer coefficient. A much better agreement is exhibited by the correlation of Cavallini and Zecchin, particularly in the range of the larger mass flow rates. This fact is not surprising if one considers that the correlation was proposed for the high velocity regime, that is in annular flow. In the calculation schemes proposed by Butterworth and by Paikert, allowance is made for the various condensation modes, namely; stratifying, annular and intermediate. It can be seen that the Paikert calculation scheme compares favourably with experimental results, whereas the Butterworth procedure does not prove satisfactory.

Figures 15 and 16 show the comparison of experimental and predicted values of pressure drops in evaporation and condensation, respectively. The correlations of Chawla [15] and Grønnerud [16] prove to be very good predictors both in evaporation and condensation. In evaporation, also the Friedel correlation [17] was tested; as can be seen, experimental data are overpredicted at low mass flow rates, whereas they are underpredicted at high mass flow rates. In condensation, a further comparison was made against Rohsenow correlation [18], that was worked out for the annular flow. The evident convergence of such predictions to the experimental data as mass flow rate is increased, points out the progressive achievement of annular flow in the test section.

The good agreement of data for the smooth tube with predicted values by several correlations among those tested, seems to represent a satisfactory reliability check of the adopted experimental procedures.

## Acknowledgements

The authors wish to thank Dr. S. Conti and Mr. S. Finetti of the Europa Metalli LMI who have built the experimental apparatus, and Mr. M. Corso and Mr. A. Trovati of the Dipartimento di Energetica who greatly helped in setting up the apparatus.

## REFERENCES

1. Bergles, A.E., 'Advanced Enhancement for Heat Exchangers'. *Proc. of The Japan-U.S. Seminar on Thermal Engineering for Global Enviromental Protection (A-5)*, pp. 1-14, San Francisco, July 1994.
2. Schlager, L.M., Pate, M.B., and Bergles, A.E., 'Evaporation and Condensation Heat Transfer and Pressure Drop in Horizontal, 12.7-mm Microfin Tubes with Refrigerant 22'. *Journal of Heat Transfer*, vol. 112, pp. 1041-1047 (1990).
3. Thome, J.R., 'Two-phase Heat Transfer to New Refrigerants'. *Proc. of the 10th IHTC*, vol. 1, pp. 19-41, Brighton, August 1994.

4. Webb, R.L., 'Advances in Modeling Enhanced Heat Transfer Surface'. *Proc. of the 10th IHTC*, vol. 1, pp. 445-459, Brighton, August 1994.
5. Gnielinski, V., 'Forced convection in ducts'. In *Handbook of Heat Exchanger Design*, Hemisphere, pp. 2.5.1/1-11 (1983).
6. Gregorig, R., 'Hautkondensation an Feingewellten Oberflächen bei Berücksichtigung der Oberflächenspannungen'. *Z. Angew. Math. Phys.*, vol. 5, pp. 36-49 (1954).
7. Kubanek, G.R., Miletti, D.L., 'Evaporative Heat Transfer and Pressure Drop of Internally-Finned Tubes with Refrigerant 22'. *Journal of Heat Transfer*, vol. 101, pp. 447-452 (1979).
8. Chawla, J.M., 'Wärmeübertragung und Druckabfall in waagerechten Rohren bei der Strömung von verdampenden Kältemitteln'. *Kältetechnik-Klimatisirung*, heft 8, pp. 246-252 (1967).
9. Liu, Z., Winterton, R.H.S., 'A General Correlation for Saturated and Subcooled Flow Boiling in Tubes and Annuli Based on Nucleate Pool Boiling'. *Int. J. Heat Mass Transfer*, vol. 34, pp.2759-2765 (1991).
10. Kandlikar, S.G., 'Flow Boiling Maps for Water, R22 and R134a in the Saturated Region'. *Proc. 9th IHTC*, vol. 2, pp. 15-20, Jerusalem, August 1990.
11. Shah, M.M., 'A General Correlation for Heat Transfer during Film Condensation inside Pipes'. *Int. J. Heat Mass Transfer*, vol. 22, pp. 547-556 (1979).
12. Cavallini, A., Zecchin, R., 'Scambio Termico nella Condensazione ad Alta Velocità di Fluidi Frigorigeni Organici entro Tubi: Dati Sperimentali e Correlazioni'. *La Termotecnica*, vol. XXVI, n. 4, pp. 199-208 (1972).
13. Butterworth, D., 'Film Condensation of Pure Vapor'. In *Handbook of Heat Exchanger Design*, Hemisphere, pp. 2.6.2/1-19 (1983).
14. Paikert, P., 'Wärmeübertragung bei Kondensation und Bemessung von Verflüssigern'. In *Handbuch der Kältetechnik*, Springer, 6ter Band/Teil B (1988).
15. VDI-Wärmeatlas, Berechnungsblätter für denWärmeübergang. 2.Aufl. Düsseldorf: VDI-Verlag (1974)
16. Grønnerud, R., 'Investigation in Liquid Hold-up, Flow Resistance and Heat Transfer in Circulation Type Evaporators', Part IV: Two-Phase resistance in Boiling Refrigerants'. *Bull. de l'Inst. du Froid*, Annexe 1972-1.
17. Hewitt, G.F., 'Gas-Liquid Flow'. In *Handbook of Heat Exchanger Design*, Hemisphere, pp. 2.3.2/1-33 (1983).
18. Griffith, P., Rohsenow, W.M., 'Condensation'. In *Handbook of Heat Transfer Fundamentals*, McGraw Hill, pp. 11/1-36 (1985).